Pergamon

Int. J. Solids Structures Vol. 33, No. 3, pp. 315–330, 1996

0020-7683/96 $9.50 + .00

0020-7683(95)00052-6

INTERACTIVE BUCKLING OF THIN-WALLED OPEN ELASTIC BEAM-COLUMNS WITH INTERMEDIATE STIFFENERS

ANDRZEJ TETER

Department of Applied Mechanics, Technical University of Lublin, PL-20-618 Lublin, ul. Nadbystrzycka 36, Poland

and

ZBIGNIEW KOLAKOWSKI

Department of Strength Materials and Structures (K12), Technical University of Łódź, PL-90-924 Łódź, ul. Stefanowskiego 1/15, Poland

(*Received* 2 *November* 1994; *in revised form* 23 *February* 1995)

Abstract—Influence of the interactive buckling on the post-buckling behaviour of thin-walled columns with imperfections is studied. This investigation is concerned with open elastic beam-columns with intermediate and edge stiffeners under axial compression and constant bending moment. The columns are assumed to be simply supported at the ends. The paper's aim is to contribute to the study of the equilibrium path in the post-buckling behaviour of imperfect structures using the first-order approximation. The present paper is the continuation of a paper by Kolakowski and Teter (1995, *Int. J. Solids Structures* **32**, 1501–1516) where the interactive buckling of thin-walled closed beam-columns with central intermediate stiffeners was considered.

NOTATION

b_i	width of the i-th wall of column,
E	Young's modulus,
h_i	thickness of the i-th wall of the column,
l	length of the column,
m	number of axial half-waves of n-th mode,
n	number of mode,
$\bar{N}$	force field,
N_{ix}, N_{iy}, N_{ixy}	in-plane stress resultants for the i-th wall,
$N_{ix}^{(n)}, N_{iy}^{(n)}, N_{ixy}^{(n)}$	in-plane stress resultants for the i-th wall in the first approximation,
$\bar{U}$	displacement field,
u_i, v_i, w_i	displacement components of middle surface of the i-th wall,
$u_i^{(n)}, v_i^{(n)}, w_i^{(n)}$	buckling displacement fields,
λ	scalar load parameter,
ν	Poisson's ratio ($\nu = 0.3$),
ξ_n	amplitude buckling mode number n,
$\bar{\xi}_n$	imperfection amplitude corresponding to ξ_n,
$\sigma_n^* = \sigma_n 10^3/E$	dimensionless stress of mode number n,
σ_m^*	min $(\sigma_1^*, \sigma_2^*, \sigma_3^*)$,
σ_ξ^*	limit dimensionless stress for imperfect column (load carrying capacity).

1. INTRODUCTION

Intermediate stiffeners are widely used in many types of metal structures. These stiffeners carry a portion of the loads and subdivide the plate element into smaller sub-elements, thus increasing considerably the load-carrying capacity.

The importance of the minimum rigidity of the intermediate stiffeners required to restrict buckling to the plate elements was studied by, for example, Desmond (1977), Höglund (1978) and Konig (1978). The test specimens, experimental works and comparisons made with design rules of plates and open cross-section structures were detailed by Hoon *et al.* (1993) and Bernard *et al.* (1993).

Turning the free edge of an unstiffened web inwards and outwards to form a "lip" can substantially improve the local buckling resistance of a member. The lip is the most common type of edge stiffener used in open thin-walled sections.

Local buckling is the major feature to be taken into account in the design of thin-walled sections. The local buckles cause reduction in the stiffness of a section and consequently lowers the load-carrying capacity relative to a non-locally buckled section. In order to improve the local buckling characteristics, edge stiffeners are widely used to stiffen the flat compressed elements of thin-walled structural members (Kolakowski, 1989: Seah *et al.*, 1993). The behaviour of plate elements of thin-walled sections stiffened by compound lips is studied.

The size and shape of intermediate stiffeners and edge stiffeners in thin-walled open structures exert a strong influence on the stability and post-buckling behaviour of the thin-walled structures.

The allowance for interactive buckling is necessary for the determination of the imperfection sensitivity of structures and of the limit load capacity close to optimum where the values of critical loads are identical, or nearly so. The asymptotic Koiter's method (Koiter, 1963, 1976) is used in the first-order approximation.

For the first-order approximation Koiter and van der Neut (1980) have proposed a technique in which the interaction of an overall mode with two local modes (three-mode approach) having the same wavelength has been considered. The fundamental local mode is henceforth called "primary" and the non-trivial higher local mode (having the same wavelength as the "primary") corresponding to the mode triggered by an overall longwave mode is called "secondary".

More comprehensive reviews of the literature concerning interactive buckling have been carried out by Ali and Sridharan (1988), Benito and Sridharan (1984–1985), Manevich (1985, 1988), Pignataro and Luongo (1987), Sridharan and Ali (1985, 1986), Sridharan and Peng (1989) and Kolakowski (1993).

In the present paper, the post-buckling behaviour of thin-walled open structures with the intermediate and edge stiffeners in the elastic range subject to axial compression and a bending moment is examined based on the method by Kolakowski and Teter (1995). In the solution obtained, the effects of interactive buckling of two local modes having the same wavelength, the shear lag phenomenon and also the effect of cross-sectional distortions are included.

Since for the first-order approximation the limit load is always lower than the minimum value of a bifurcational load obtained in the linear analysis, this approximation can be used as a lower bound estimation of a load-carrying capacity.

2. STRUCTURAL PROBLEM

The long thin-walled prismatic open beam-columns with intermediate stiffeners simply supported at both ends are considered.

A plate model is adopted for the beam-column. For the ith wall precise geometrical relationships are assumed to take into account both out-of-plane and in-plane bending (Kolakowski and Teter, 1995):

$$\begin{aligned}
\varepsilon_{ix} &= u_{i,x} + 0.5(u_{i,x}^2 + v_{i,x}^2 + w_{i,x}^2),\\
\varepsilon_{iy} &= v_{i,y} + 0.5(u_{i,y}^2 + v_{i,y}^2 + w_{i,y}^2),\\
2\varepsilon_{ixy} &= \gamma_{ixy} = u_{i,y} + v_{i,x} + u_{i,x}u_{i,y} + v_{i,x}v_{i,y} + w_{i,x}w_{i,y},\\
\kappa_{ix} &= -w_{i,xx}, \quad \kappa_{iy} = -w_{i,yy}, \quad \kappa_{ixy} = -w_{i,xy}.
\end{aligned} \tag{1}$$

The differential equilibrium equations resulting from the virtual work principle and corresponding to expressions (1) for the ith wall can be written as follows:

$$\begin{aligned}
&N_{ix,x} + N_{ixy,y} + (N_{ix}u_{i,x})_{,x} + (N_{iy}u_{i,y})_{,y} + (N_{ixy}u_{i,x})_{,y} + (N_{ixy}u_{i,y})_{,x} = 0,\\
&N_{iy,y} + N_{ixy,x} + (N_{ix}v_{i,x})_{,x} + (N_{iy}v_{i,y})_{,y} + (N_{ixy}v_{i,x})_{,y} + (N_{ixy}v_{i,y})_{,x} = 0,
\end{aligned} \tag{2}$$

$$D_i\nabla\nabla w_i - (N_{ix}w_{i,x})_{,x} - (N_{iy}w_{i,y})_{,y} - (N_{ixy}w_{i,y})_{,x} - (N_{ixy}w_{i,x})_{,y} = 0,$$

The solution of these equations for each plate should satisfy kinematic and static conditions at the junctions of adjacent plates and boundary conditions at the ends $x = 0$ and $x = l$, where l is length.

The non-linear problem is solved by the asymptotic Byskov and Hutchinson method (1977). Displacement $\bar{U}$ and force fields $\bar{N}$ are expanded in power series in the buckling mode amplitudes, ξ_n (divided on the thickness of the first component plate), with regard to the imperfections of the buckling modes with amplitudes $\bar{\xi}_n$:

$$\begin{aligned}\bar{U} &= \lambda\bar{U}_i^{(0)} + \xi_n\bar{U}_i^{(n)} + \cdots + \bar{\xi}_n\bar{U}_i^{(n)},\\ \bar{N} &= \lambda\bar{N}_i^{(0)} + \xi_n\bar{N}_i^{(n)} + \cdots + \bar{\xi}_n\bar{N}_i^{(n)},\end{aligned} \tag{3}$$

The numerical difficulties connected with a convergance of the problem presented for the first-order approximation induce the necessity of introducing new orthogonal functions in the sense of boundary conditions of the first order on two longitudinal edges [for details see Kolakowski and Teter (1995)].

Regarding the above, the first-order approximation of the system of homogeneous differential equations with respect to the new function and appropriate junction conditions for adjacent plates is solved by the transition matrices method. The numerical integration of the equilibrium equations in the transverse direction is used in order to obtain a relation between state vectors on two longitudinal edges applying the Godunov orthogonalization method.

3. ANALYSIS OF RESULTS

The long thin-walled prismatic beam-columns of open cross-section [Fig. 1(a)], reinforced with V-shaped [Figs 1(b–h)] and C-shaped [Fig. 1(i)] intermediate stiffeners, have been formed. Intermediate stiffeners have been built of plates whose width is b_s. Detailed numerical calculations have been carried out for several cross-sectional reinforcements of thin-walled beam-columns subject to uniform and eccentric compression.

In pre-buckling state the beam-column is subjected to linearly variable stresses caused by axial forces and bending moments which are dealt with as external loads. The load distribution can be described with the ratio of stress $p_j(y)$ at point j of the cross-section to the greatest compressive stress, $p_{max} = p_1$ applied to the flange (Fig. 1). In the present paper the load distribution is defined by the ratio of stresses at point 2 to the maximum stresses at point 1, $\kappa = p_2/p_{max} = p_2/p_1$. Stress p_j is considered positive if it is a compressive stress. In order to compare load capacities of different cross-sections (Fig. 1), identical distributions of external stress are assumed: this implies a change in the values of compressive force and bending moment.

In all the cases considered the three-mode approach can be taken into account.

The calculations are carried out for a beam-column of the following constant geometrical dimensions [Figs 1(a–i)]:

$$h_1/b_2 = 2.0 \quad h_1/b_3 = 1.0 \quad l/b_1 = 13.0 \quad b_1/h_1 = 50$$

and for the other dimensions of cross-section which are, respectively:
Figs 1(c–h)

$$h_3/b_1 = 0.25 \quad h_3/h_1 = 1.0;$$

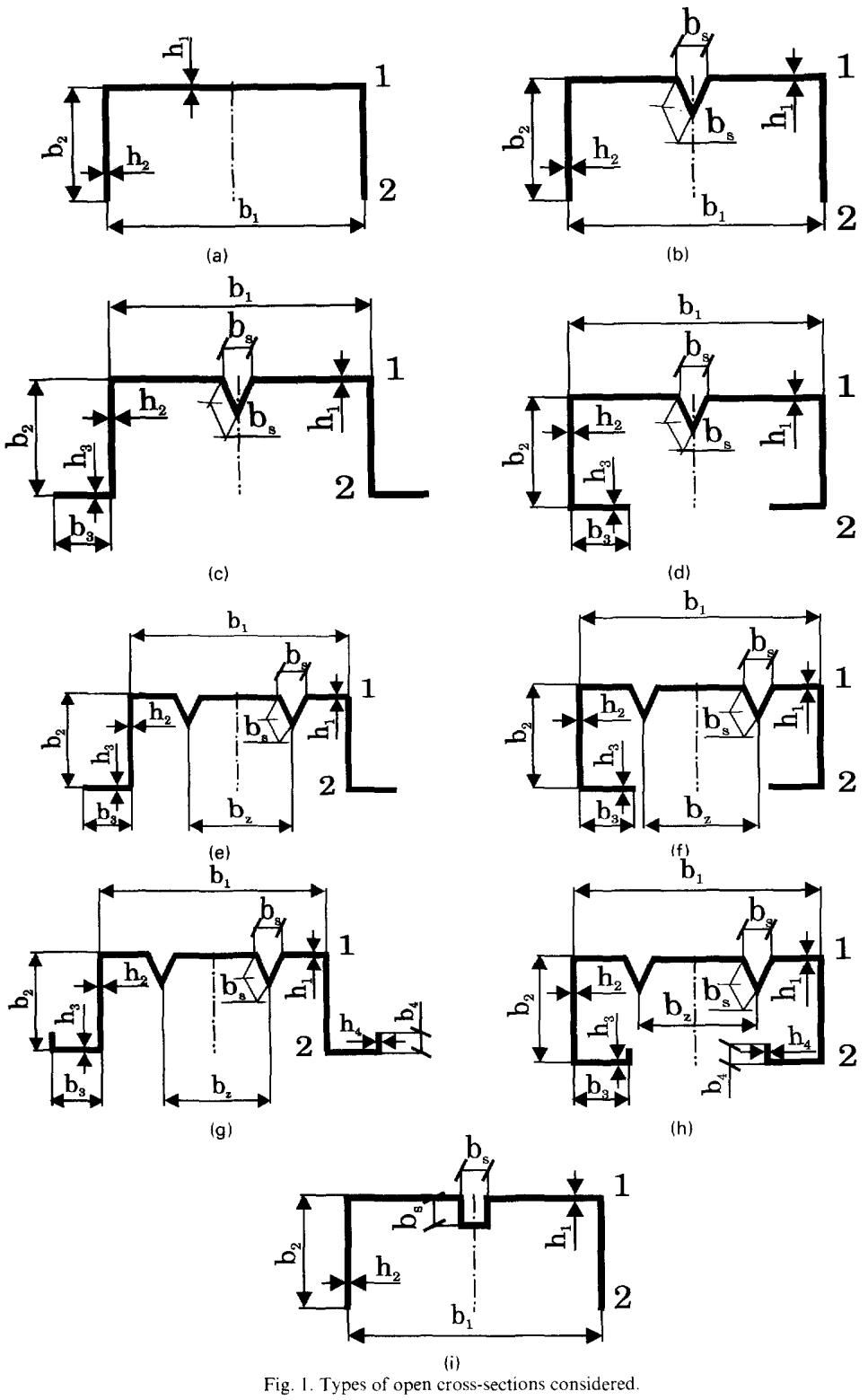

Fig. 1. Types of open cross-sections considered.

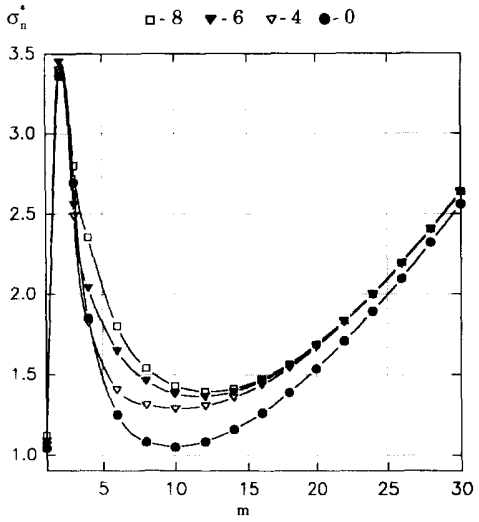

Fig. 2. Dimensionless stress σ_n^* carried by the number of half-waves m for a uniformly compressed column with the cross-section presented in Fig. 1(b).

Figs 1(g, h)

$$b_4/b_1 = 0.1 \quad h_4/h_1 = 1.0 \quad b_2/b_1 = 0.24.$$

Intermediate stiffeners are modelled with plates, their dimensions being $b_s/h_1 = \{2, 4, 6, 8\}$. Figures 2–9 present dimensionless critical stress σ_n^* (where the index n takes the value 1 in the overall mode, 2 in the primary local mode and 3 in the secondary local one) as a function of the number of half-waves, m, for the above values of b_s/h_1. As a comparison, the results are shown as obtained for a "smooth" column [i.e. $b_s/h_1 = 0$, Figs 2(0)–9(0)].

For the channel section without intermediate and edge stiffeners [Fig. 1(a)] the ratio of the flexural–torsional (primary global) stress to the primary local stress is found here to be equal to 0.99 and the ratio of the purely flexural (secondary global) stress to the primary local stress is determined to be equal to 1.42 [see Kolakowski (1989, 1993) for a more detailed analysis].

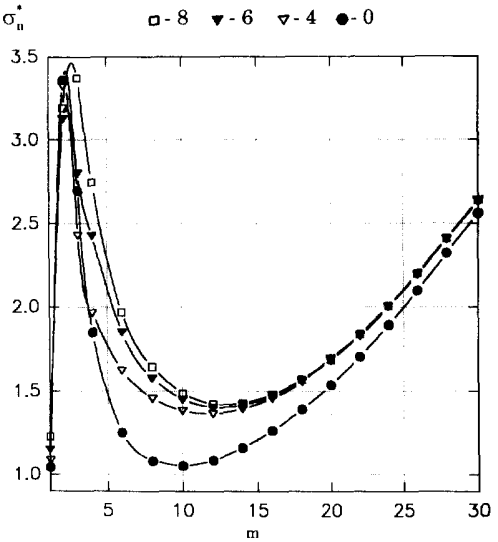

Fig. 3. Dimensionless stress σ_n^* carried by the number of half-waves m for a uniformly compressed column with the cross-section presented in Fig. 1(i).

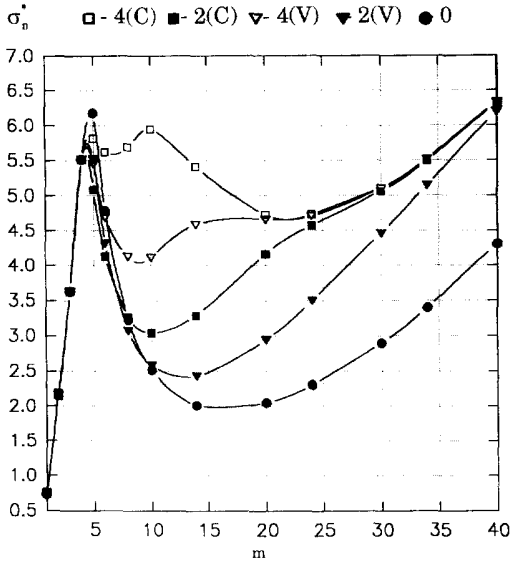

Fig. 4. Dimensionless stress σ_n^* carried by the number of half-waves m for a uniformly compressed column with the cross-section presented in Fig. 1(c).

Reinforcing the above channel section with the V- or C-shaped intermediate stiffeners causes an increase in the values of the local critical stresses by about 35% at $b_s/h_1 = 6$ and 8 while the values of the global critical stresses do not increase significantly (by approximately 10%) (Figs 2 and 3). For this channel section with $b_s/h_1 \geqslant 6$, the shape and the size of the intermediate stiffeners do not contribute practically to any increase in the critical stress values.

The introduction of intermediate stiffeners increases the flexural rigidity of plate elements and, consequently, also the local critical stress values. In these cases the webs are the elements responsible for the local stability loss. Global critical stress values for all analysed types of intermediate stiffeners remain virtually unchanged because of small variations in the moment of inertia of the cross-section.

In all cases analysed the flexural–torsional buckling precedes the purely flexural one; an exception is made by the eccentric compression of the stiffener channel section [Figs 1(d, f, h)]. It is necessary, therefore, to reinforce the cross-section with edge stiffeners. An

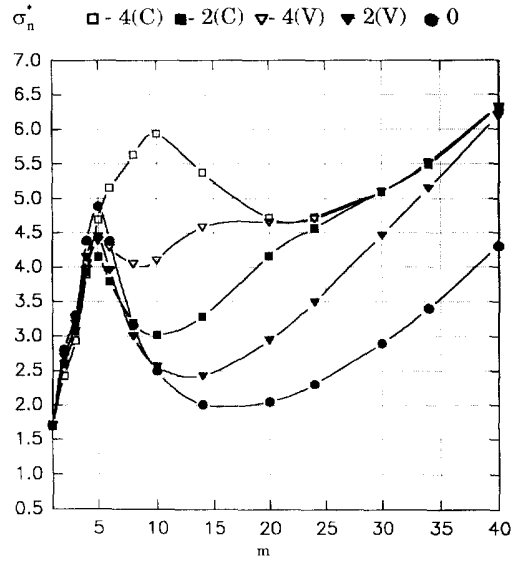

Fig. 5. Dimensionless stress σ_n^* carried by the number of half-waves m for a uniformly compressed column with the cross-section presented in Fig. 1(d).

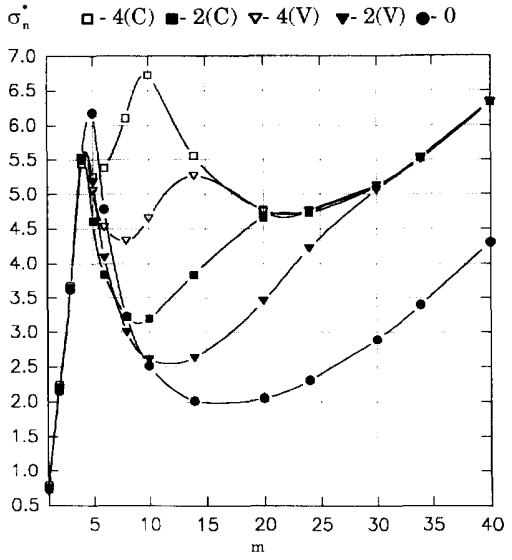

Fig. 6. Dimensionless stress σ_n^* carried by the number of half-waves m for a uniformly compressed column with the cross-section presented in Fig. 1(e).

analysis of the influence of such reinforcements (although intermediate stiffeners are not taken into account) on the critical load values was presented by Kolakowski (1989).

Columns reinforced with intermediate stiffeners and compound lip(s) may show two local minima for two different local buckling modes (Figs 4–9). The first one refers to the smaller number of half-waves, m (m = 5–12), and the second one to the greater number of half-waves (m = 20–35) as compared with the column without intermediate stiffeners. In particular cases the values of these minima for local buckling modes can differ from each other insignificantly [Figs 4(4)–9(4) for V- and C-shaped intermediate stiffener]. Each minimum, however, corresponds to a different local buckling mode. The local buckling modes referring to these two minima for the column with a V-shaped stiffener ($b_s/h_1 = 4$) under uniform compression ($\kappa = 1$) [Fig. 1(c)] are shown in Figs 10 and 11. Special attention should be paid to the fact that critical stress values referring to the second minimum are nearly equal for both local modes. In the paper of Bernard *et al.* (1993) the local buckling modes presented in Figs 10 and 11 are named as follows: $\sigma_2^* = 4.0814$ ($m = 9$), local

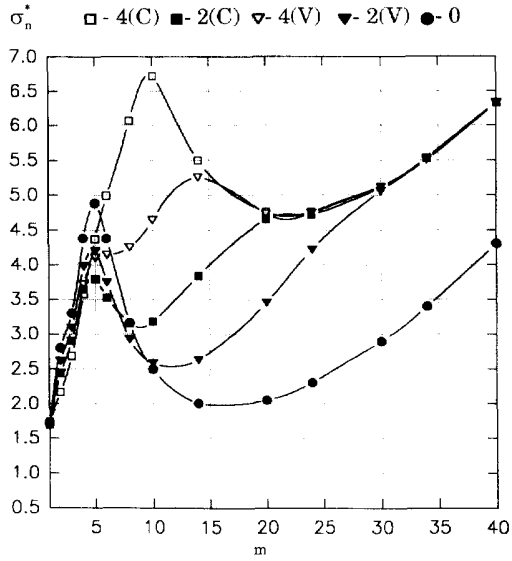

Fig. 7. Dimensionless stress σ_n^* carried by the number of half-waves m for a uniformly compressed column with the cross-section presented in Fig. 1(f).

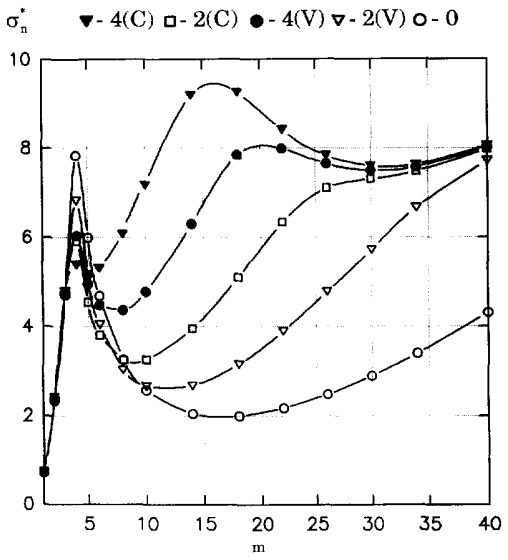

Fig. 8. Dimensionless stress σ_n^* carried by the number of half-waves m for a uniformly compressed column with the cross-section presented in Fig. 1(g).

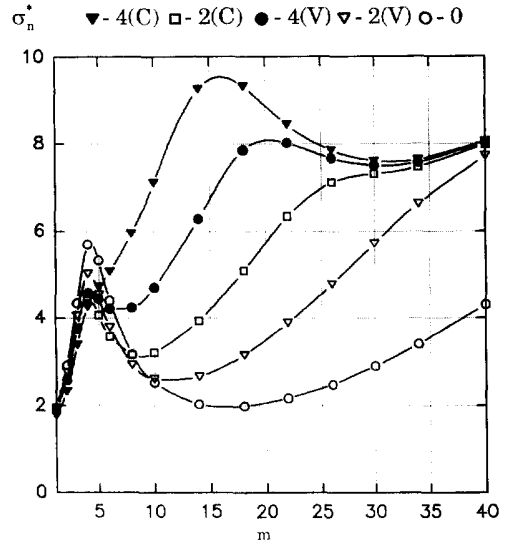

Fig. 9. Dimensionless stress σ_n^* carried by the number of half-waves m for a uniformly compressed column with the cross-section presented in Fig. 1(h).

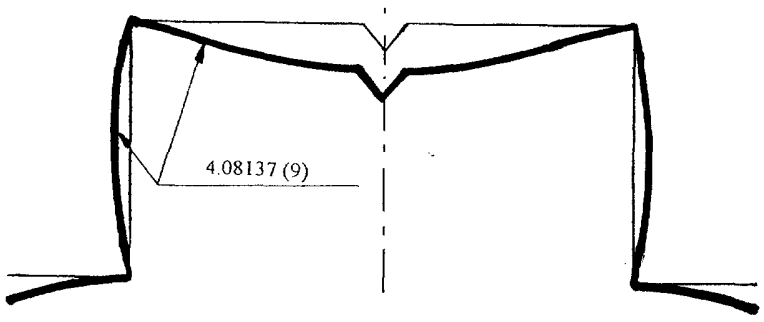

Fig. 10. Local mode at $m = 8$ under a uniform compression column.

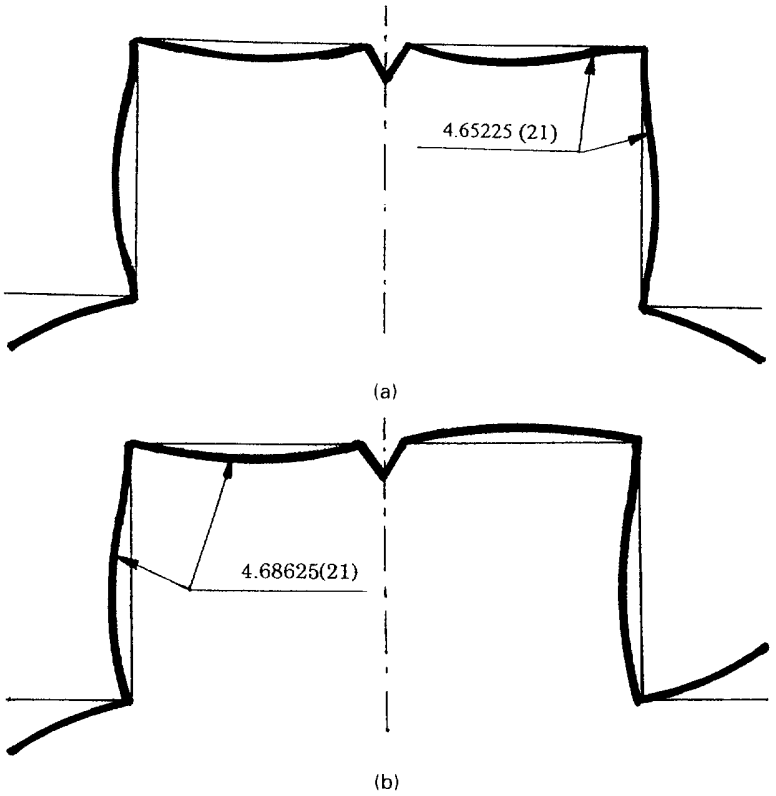

Fig. 11. Two local modes at $m = 21$ under a uniform compression column.

distortional buckling mode (Fig. 10); $\sigma_2^* = 4.6523$ ($m = 21$), local symmetric mode [Fig. 11(a)]; and $\sigma_3^* = 4.6863$ ($m = 21$), local antisymmetric mode [Fig. 11(b)].

Figure 4 and 6 compared with Figs 5 and 7 show that the introduction of the second intermediate stiffener has practically no effect on the values of the global and the local critical stresses. Hence, in the assumed geometrical configuration, the second stiffener is not needed.

The introduction of compound lips [Figs 1(g, h)] causes a marked increase in the local stresses, σ_2^*, corresponding to the second local minimum ($m = 30$–35) as well as small variations of the global stresses, σ_1^* (compare Figs 6 and 8, 7 and 9).

In the case of axial compression the introduction of outside edge stiffeners in the so-called top-hat section [Figs 1(c, e, g)] reduces (by up to 35%) the flexural–torsional critical load in comparison with the channel section [Fig. 1(a)] (compare Figs 2, 4, 6, 8); it happens through a decreased rigidity of section deplanation. Building the inside stiffeners (channel section) [Figs 1(d, f, h)] increases significantly the value of the flexural–torsional stress by increasing the deplanation rigidity (compare Figs 2, 5, 7, 9). Edge stiffeners (inside or outside) have a far weaker influence on the critical flexural stress (compare cases 2 in Tables 2 and 3, 4 and 5).

For sections stiffened by compound lips the values of the local stress remain virtually constant, their changes being practically negligible. This fact can be explained in the following way. While determining approximate values of load corresponding to the local modes under conditions of mating, we are able to take into account only the situation where the angle is constant and the bending moments are equal; moreover, the deflection function w_i for individual plates is assumed to be zero at the points of the junction [see Kolakowski (1989)].

Figures 12–19, analogous to Figs 2–9, show the dependences of the lowest dimensionless critical stresses, σ_{ii}^*, for beam-columns subjected to eccentric compression ($\kappa = 0$).

In the case of eccentric compression ($\varkappa = 0$) of the C-shaped column without intermediate stiffener [Fig. 1(a)], the ratio of the global (flexural–torsional) stress to the local

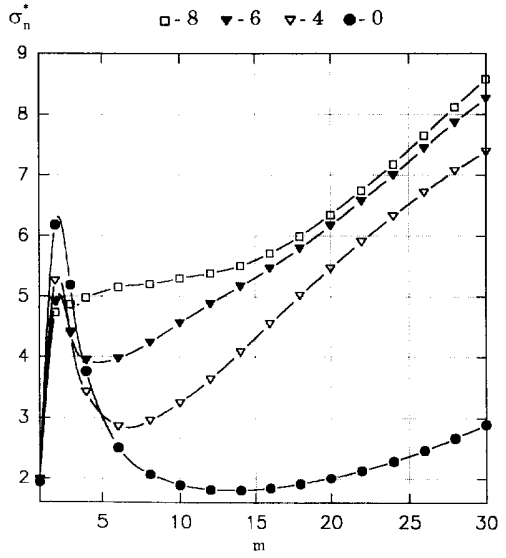

Fig. 12. Dimensionless stress σ_n^* carried by the number of half-waves m for an eccentrically compressed column ($\kappa = 0$) with the cross-section presented in Fig. 1(b).

stress is 1.065 while the ratio of the flexural stress to the local stress is 1.095. In the case of the channel section under discussion [Figs 1(a, b, i)] the local critical stress, σ_2^*, rises significantly (compare Figs 2 and 12, and 3 and 13) because of a considerable increase in stability factors of the flange compressed eccentrically which determine the stability loss.

In the case of the sections with edge stiffeners [Figs. 1(c–h)] an increased eccentricity of the compressive force may cause a slight growth of the critical load, σ_2^*, corresponding to the local distortional buckling mode. However, it causes a marked increase in σ_2^* at the second minimum referring to the local antisymmetric mode or the local symmetric mode, whereas the flexural and the flexural–torsional critical stresses, σ_1^*, have nearly doubled (compare Figs 4 and 14, 5 and 15, 6 and 16, 7 and 17, 8 and 18, and 9 and 19).

Under eccentric compression ($\kappa = 0$) the outside edge stiffener causes a slight increase in load, σ_1^* (compare Figs 12, 14, 16 and 18), while the inside one gives rise to a significant (even double) growth of the load, σ_1^*, as compared with the channel section (compare Figs 12, 15, 17 and 19).

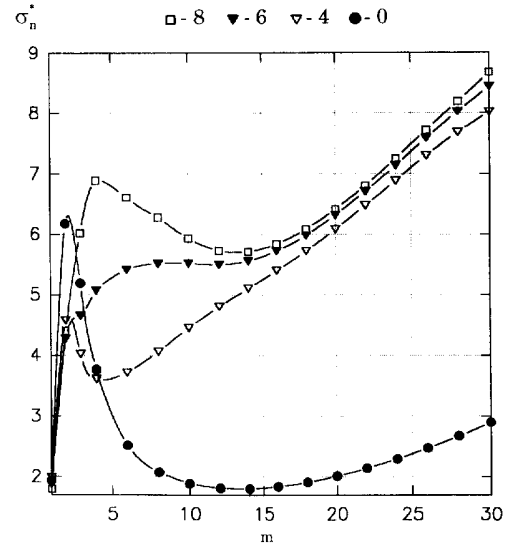

Fig. 13. Dimensionless stress σ_n^* carried by the number of half-waves m for an eccentrically compressed column ($\kappa = 0$) with the cross-section presented in Fig. 1(i).

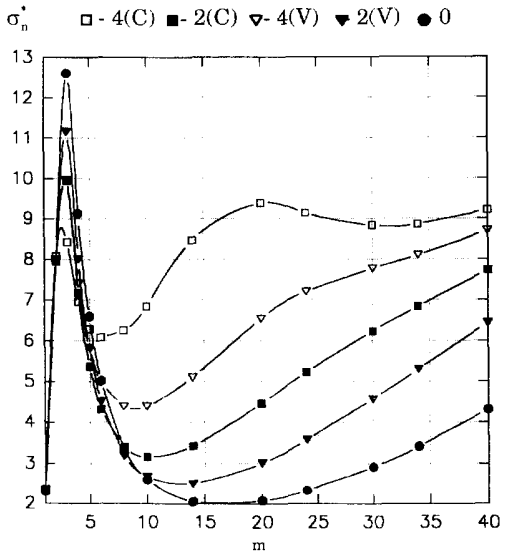

Fig. 14. Dimensionless stress σ_n^* carried by the number of half-waves m for an eccentrically compressed column ($\kappa = 0$) with the cross-section presented in Fig. 1(c).

Detailed numerical calculations aimed at the determination of the load-carrying capacity of the structures σ_s^* are carried out for the column discussed having assumed the following imperfections $|\bar{\xi}_1| = 1.0$, $|\bar{\xi}_2| = 0.2$, $\bar{\xi}_3 = 0.0$.

In each case the signs of the imperfections have been chosen in the most unfavourable fashion, i.e. so that σ_s^* would assume its minimum value [see, for example, Kolakowski (1989) for a more detailed discussion]. The local imperfections always promote an interaction between the local modes and the global mode.

Tables 1–5 present the number of half-waves, m, the values of dimensionless critical stresses, σ_n^*, the limit load capacity σ_s^* in the first non-linear approximation and the load-carrying capacity to the minimum critical stress ratios, σ_s^*/σ_m^*, for a V-stiffened beam-columns, its dimensions being $b_s/h_1 = \{2, 4, 6, 8\}$. The cases of uniform ($\kappa = 1$) and eccentric ($\kappa = 0$) compression are analysed. The following code has been used in Tables 1–5 in order to identify the support conditions on the axis of the symmetry of the cross-section: A, antisymmetry: S, symmetry, respectively, for the nth buckling mode.

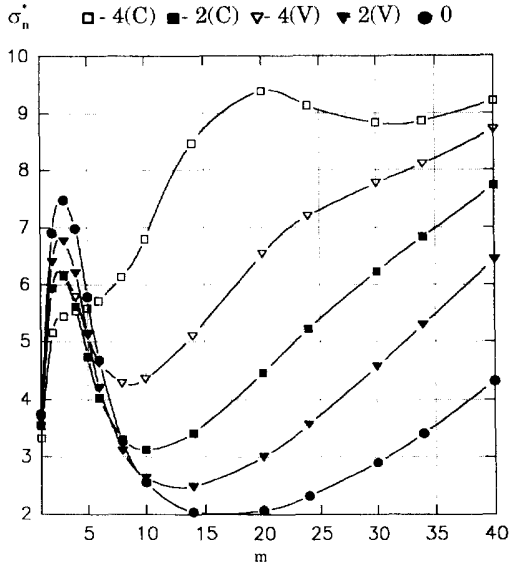

Fig. 15. Dimensionless stress σ_n^* carried by the number of half-waves m for an eccentrically compressed column ($\kappa = 0$) with the cross-section presented in Fig. 1(d).

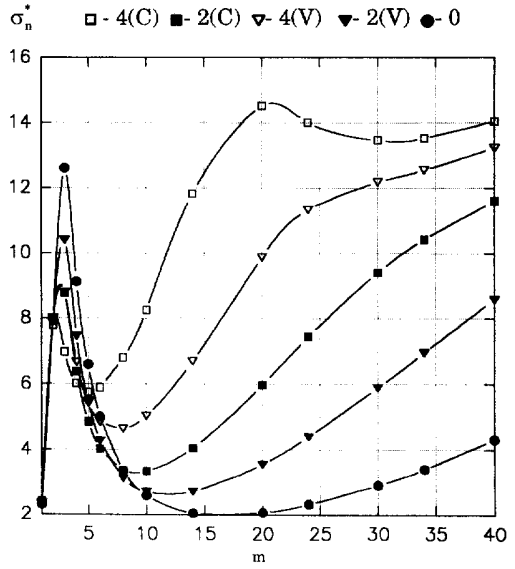

Fig. 16. Dimensionless stress σ_n^* carried by the number of half-waves m for an eccentrically compressed column ($\kappa = 0$) with the cross-section presented in Fig. 1(e).

It is evident that when critical stress values become close to each other, the imperfection sensitivity increases. A decrease of limit load in the presence of imperfections is very significant, especially if local imperfections are present. Attention should be paid to the proper selection of local buckling modes (compare cases 1 and 2, 3 and 4, 5 and 6, and 7 and 8 in Table 1). This can be accomplished only by means of non-linear analysis [see Kolakowski and Teter (1995) for a more detailed analysis].

From these data it can be concluded that the interaction of the flexural–torsional (primary global) buckling mode with the local distortional mode (cases 5 in Tables 2–4) and the interaction of the same global mode with the local symmetric mode (cases 6 in Tables 2–4) give nearly the same value of load-carrying capacity σ_s^*. These interactions of the above modes are more dangerous than the interaction of the global one with the localantisymmetric mode for the three-mode approach; but on the another hand the interaction of the secondary global (flexural) mode with the local symmetric mode gives

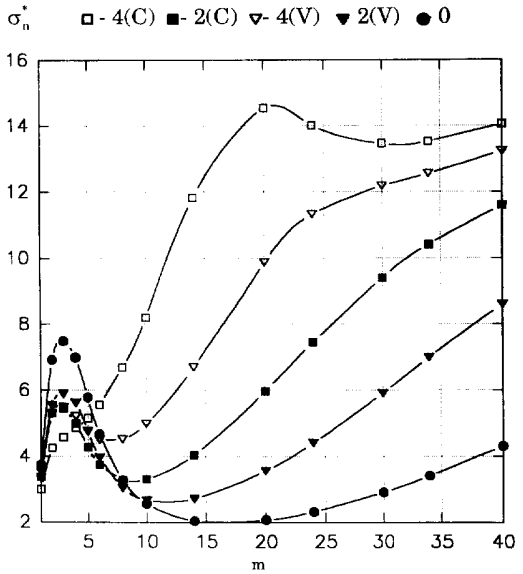

Fig. 17. Dimensionless stress σ_n^* carried by the number of half-waves m for an eccentrically compressed column ($\kappa = 0$) with the cross-section presented in Fig. 1(f).

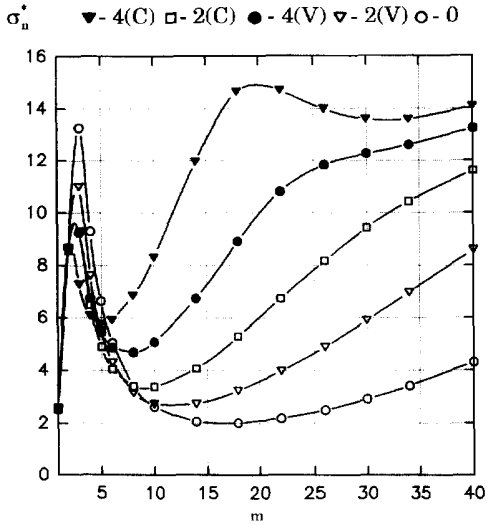

Fig. 18. Dimensionless stress σ_n^* carried by the number of half-waves m for an eccentrically compressed column ($\kappa = 0$) with the cross-section presented in Fig. 1(g).

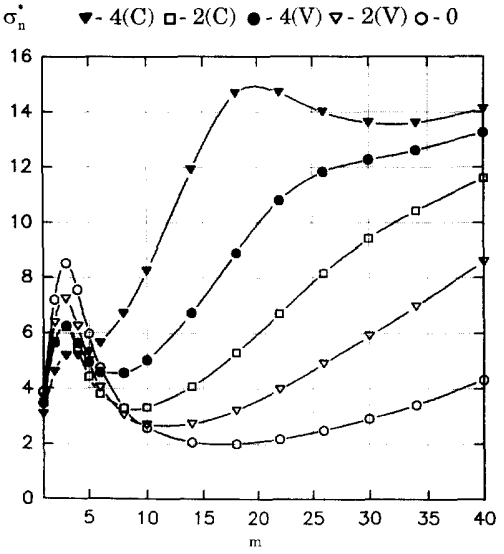

Fig. 19. Dimensionless stress σ_n^* carried by the number of half-waves m for an eccentrically compressed column ($\kappa = 0$) with the cross-section presented in Fig. 1(h).

Table 1. Load-carrying capacity for a beam-column with the cross-section presented in Fig. 1(b) at imperfections $|\bar{\xi}_1| = 1.0$, $|\bar{\xi}_2| = 0.2$, $\bar{\xi}_3 = 0.0$

	b_s/h_1	m	κ	σ_1^*	σ_2^*	σ_3^*	σ_S^*	σ_S^*/σ_m^*
1	0	10	1	1.04272(A)	1.05130(S)	1.43995(A)	0.74597	0.7154
2	0	10	1	1.48925(S)	1.05130(S)	3.30787(S)	0.66064	0.6284
3	4	10	1	1.06017(A)	1.28680(S)	1.43683(A)	0.81008	0.7641
4	4	10	1	1.42665(S)	1.28680(S)	4.76868(S)	0.74390	0.5781
5	6	12	1	1.08354(A)	1.36419(S)	1.38694(A)	0.81211	0.7495
6	6	12	1	1.38114(S)	1.36419(S)	8.23209(S)	0.73694	0.5402
7	8	12	1	1.11805(A)	1.39357(S)	1.40416(A)	0.83306	0.7451
8	8	12	1	1.33416(S)	1.39357(S)	12.1086(S)	0.74086	0.5553
9	0	13	0	1.92083(A)	1.80274(S)	5.17058(A)	1.50565	0.8352
10	0	13	0	1.97391(S)	1.80274(S)	6.70560(S)	1.28355	0.7120
11	4	6	0	1.87637(S)	2.83379(S)	13.5828(S)	1.50579	0.8025
12	4	6	0	1.94241(A)	2.83379(S)	8.61861(A)	1.78274	0.9178
13	6	5	0	1.81973(S)	3.82562(S)	16.5073(S)	1.59590	0.8770
14	6	5	0	1.98190(A)	3.82562(S)	10.5496(A)	1.81859	0.9176

Table 2. Load-carrying capacity for a beam-column with the cross-section presented in Fig. 1(c) at imperfections $|\bar{\xi}_1| = 1.0$, $|\bar{\xi}_2| = 0.2$, $\bar{\xi}_3 = 0.0$

	b_s/h_1	m	κ	σ_1^*	σ_2^*	σ_3^*	σ_S^*	σ_S^*/σ_m^*
1	0	16	1	0.73056(A)	1.95939(S)	8.97405(A)	0.71997	0.9855
2	0	16	1	2.41735(S)	1.95939(S)	5.27208(S)	1.27027	0.6483
3	2	13	1	0.73340(A)	2.40884(S)	5.75343(A)	0.72404	0.9872
4	2	13	1	2.40336(S)	2.40884(S)	6.13873(S)	1.56061	0.6493
5	4	9	1	0.74217(A)	4.08137(S)	8.44150(A)	0.73119	0.9852
6	4	21	1	0.74217(A)	4.65225(S)	4.68625(A)	0.73709	0.9932
7	4	9	1	2.36991(S)	4.08137(S)	9.33738(S)	2.08030	0.8778
8	4	21	1	2.36991(S)	4.65225(S)	6.69808(S)	2.01478	0.8502
9	0	16	0	2.30788(A)	1.98661(S)	8.80586(A)	1.82024	0.9163
10	0	16	0	4.07697(S)	1.98661(S)	20.0680(S)	1.37763	0.6935
11	2	13	0	2.30597(A)	2.47374(S)	11.2848(A)	2.10503	0.9129
12	2	13	0	4.00613(S)	2.47374(S)	24.6217(S)	1.78049	0.7196
13	4	9	0	2.32384(A)	4.34292(S)	18.9132(A)	2.26433	0.9744
14	4	9	0	3.91642(S)	4.34292(S)	38.3624(S)	3.03595	0.7752

Table 3. Load-carrying capacity for a beam-column with the cross-section presented in Fig. 1(d) at imperfections $|\bar{\xi}_1| = 1.0$, $|\bar{\xi}_2| = 0.2$, $\bar{\xi}_3 = 0.0$

	b_s/h_1	m	κ	σ_1^*	σ_2^*	σ_3^*	σ_S^*	σ_S^*/σ_m^*
1	0	16	1	1.69670(A)	1.95709(S)	8.81250(A)	1.56074	0.9199
2	0	16	1	2.23318(S)	1.95709(S)	5.25127(S)	1.24935	0.6384
3	2	13	1	1.69385(A)	2.40271(S)	11.2543(A)	1.61683	0.9545
4	2	13	1	2.19738(S)	2.40271(S)	6.07771(S)	1.57388	0.7163
5	4	9	1	1.69931(A)	4.04368(S)	8.33568(A)	1.66776	0.9814
6	4	21	1	1.69931(A)	4.64486(S)	4.68072(A)	1.60440	0.9441
7	4	9	1	2.14159(S)	4.04368(S)	8.92696(S)	2.02503	0.9456
8	4	21	1	2.14159(S)	4.64486(S)	6.69583(S)	1.96122	0.9158
9	0	16	0	3.74445(S)	1.98329(S)	20.0011(S)	1.37181	0.6917
10	0	16	0	4.41695(A)	1.98329(S)	8.76704(A)	1.89695	0.9565
11	2	13	0	3.64742(S)	2.46371(S)	24.5641(S)	1.80301	0.7318
12	2	13	0	4.37564(A)	2.46371(S)	11.1876(A)	2.26962	0.9212
13	4	8	0	3.53495(S)	4.27370(S)	44.5287(S)	3.00277	0.8495
14	4	8	0	4.36246(A)	4.27370(S)	21.3107(A)	3.97268	0.9296

Table 4. Load-carrying capacity for a beam-column with the cross-section presented in Fig. 1(e) at imperfections $|\bar{\xi}_1| = 1.0$, $|\bar{\xi}_2| = 0.2$, $\bar{\xi}_3 = 0.0$

	b_s/h_1	m	κ	σ_1^*	σ_2^*	σ_3^*	σ_S^*	σ_S^*/σ_m^*
1	0	16	1	0.73056(A)	1.95939(S)	8.97405(A)	0.71995	0.9855
2	0	16	1	2.41735(S)	1.95939(S)	5.27208(S)	1.27029	0.6483
3	2	12	1	0.73777(A)	2.53665(S)	6.14809(A)	0.73429	0.9953
4	2	12	1	2.38862(S)	2.53665(S)	6.60829(S)	1.65195	0.6916
5	4	7	1	0.75485(A)	4.32935(S)	11.4499(A)	0.73979	0.9801
6	4	22	1	0.75485(A)	4.72035(S)	4.72147(A)	0.75173	0.9959
7	4	7	1	2.32208(S)	4.32935(S)	12.5393(S)	2.06377	0.8888
8	4	22	1	2.32208(S)	4.72035(S)	9.15358(S)	1.98494	0.8548
9	0	16	0	2.30788(A)	1.98661(S)	8.80586(A)	1.82024	0.9163
10	0	16	0	4.07697(S)	1.98661(S)	20.0680(S)	1.37763	0.6935
11	2	12	0	2.30410(A)	2.61646(S)	11.5126(A)	2.18241	0.9472
12	2	12	0	3.93972(S)	2.61646(S)	27.4927(S)	1.92227	0.7347
13	4	7	0	2.33600(A)	4.63363(S)	22.9795(A)	2.21012	0.9461
14	4	7	0	3.77149(S)	4.63363(S)	49.1891(S)	3.13993	0.8325

Table 5. Load-carrying capacity for a beam-column with the cross-section presented in Fig. 1(f) at imperfections $|\bar{\xi}_1| = 1.0$, $|\bar{\xi}_2| = 0.2$, $\bar{\xi}_3 = 0.0$

	b_2/h_1	m	κ	σ_1^*	σ_2^*	σ_3^*	σ_s^*	σ_s^*/σ_m^*
1	0	16	1	1.69670(A)	1.95709(S)	8.81250(A)	1.56074	0.9199
2	0	16	1	2.23318(S)	1.95709(S)	5.25127(S)	1.24935	0.6384
3	2	12	1	1.69553(A)	2.52731(S)	6.14180(A)	1.67189	0.9861
4	2	12	1	2.16433(S)	2.52731(S)	6.51667(S)	1.66843	0.7709
5	4	22	1	1.70854(A)	4.71002(S)	4.71164(A)	1.60454	0.9391
6	4	22	1	2.05977(S)	4.71002(S)	9.18548(S)	1.89370	0.9194
7	0	16	0	3.74445(S)	1.98329(S)	20.0011(S)	1.37181	0.6917
8	0	16	0	4.41695(A)	1.98329(S)	8.76704(A)	1.89695	0.9565
9	2	12	0	3.53158(S)	2.60405(S)	26.2028(S)	1.96924	0.7562
10	2	12	0	3.99161(A)	2.60405(S)	11.4392(A)	2.32386	0.8924
11	4	7	0	3.35527(S)	4.44860(S)	51.2227(S)	2.93559	0.8749
12	4	7	0	4.31999(A)	4.44860(S)	21.3367(A)	3.85839	0.8931

the smallest values of the ratio σ_s^*/σ_m^* for the interaction of buckling modes considered (Tables 1–5).

In the case of eccentric compression the global stress values, σ_1^*, are significantly higher than under uniform compression while the limit stress values, σ_s^*/σ_m^* are less (compare, for example, cases 5, 6, 7, 8, 13 and 14 in Tables 2–4); this means that the imperfection sensitivity increases together with the eccentricity of the compressive force.

In all the cases investigated the channel sections have a higher load capacity, σ_s^*, than the top-hat sections (compare Tables 2–5); therefore inside lips are more effective than outside ones.

The theory presented here enables an analysis of all buckling modes for intermediate and edge stiffeners of different shapes and flexural rigidities to be carried out; this can help in their rational design.

Results obtained for intermediate C-stiffeners are analogous to V-stiffeners.

4. CONCLUSIONS

The interactive buckling analysis of thin-walled open beam-columns with intermediate and edge stiffeners under axial compression and a constant bending moment carried out by means of the transition matrix method has been presented. Global and local modes are described by plate theory. Intermediate and edge stiffeners are found to exert a strong influence on the local buckling modes and the load-carrying capacity.

The present analysis has to be completed by including the second approximation in order to investigate post-buckling when the first-order of the interaction is weak.

REFERENCES

Ali, M. A. and Sridharan, S. (1988). A versatile model for interactive buckling of columns and beam-columns. *Int. J. Solids Structures* **24**, 481–486.

Benito, R. and S. Sridharan, S. (1984–1985). Mode interaction in thin-walled structural members. *J. Struct. Mech.* **12**, 517–542.

Bernard, E. S., Bridge, R. Q. and Hancock, G. J. (1993). Tests of profiled steel decks with V-stiffeners. *J. Struct. Engng* **119**, 2277–2293.

Byskov, E. and Hutchinson, J. W. (1977). Mode interaction in axially stiffened cylindrical shells. *AIAA Journal* **15**, 941–948.

Desmond, T. P. (1977). The behaviour and strength of thin-walled compression members with longitudinal stiffeners. Department of Structural Engineering Report No. 369, Cornell University.

Hoon, K. H., Rhodes, J. and Seah, L. K. (1993). Tests on intermediately stiffened plate elements and beam compression elements. *Thin-walled Structures* **16**, 111–143.

Höglund, T. (1978). *Design of Trapezoidal Sheeting Provided with Stiffeners in the Flanges and Webs*. Manus Stockholm, Sweden.

Koiter, W. T. (1963). Elastic stability and post-buckling behaviour. In *Proceedings of the Symposium on Nonlinear Problems*, University of Wisconsin Press, Wisconsin, pp. 257–275.

Koiter, W. T. (1976). General theory of mode interaction in stiffened plate and shell structures. WTHD Report 590, Delft, 41 pp.

Koiter, W. T. and van der Neut, A. (1980). Interaction between local and overall buckling of stiffened compression panels. In *Thin-walled Structures* (Edited by J. Rhodes and A. G. Walker), part I, pp. 51–56, part II, pp. 66–86, Granada, St Albans.

Kolakowski, Z. (1989a). Interactive buckling of thin-walled beams with open and closed cross-section. *Engng Trans.* **37,** 375–397.

Kolakowski, Z. (1993). Influence of modification of boundary conditions on load carrying capacity in thin-walled columns in the second order approximation. *Int. J. Solids Structures* **30,** 2597–2609.

Kolakowski, Z. and Teter, A. (1994). Interactive buckling of thin-walled closed elastic beam-columns with intermediate stiffeners. *Int. J. Solids Structures.* **32,** 1501–1516.

Konig, L. (1978). Transversely loaded thin-walled C-shaped panels with intermediate stiffeners. Document D7, Swedish Council for Building Research, Sweden.

Manevich, A. I. (1985). Stability of shells and plates with T-section stiffeners. *Stroitel. Mekh. Raschet Sooruzhenii* **2,** 34–38 (in Russian).

Manevich, A. I. (1988). Interactive buckling of stiffened plate under compression. *Mekh. Tverd. Tela* **5,** 152–159 (in Russian).

Pignataro, M. and Luongo, A. (1987). Asymmetric interactive buckling of thin-walled columns with initial imperfection. *Thin-walled Structures* **3,** 365–386.

Seah, L. K., Rhodes, J. and Lim, B. S. (1993). Influence of lips on thin-walled sections. *Thin-walled Structures* **16,** 145–177.

Sridharan, S. and Ali, M. A. (1985). Interactive buckling in thin-walled beam-columns. *J. Engng Mech. ASCE* **111,** 1470–1486.

Sridharan, S. and Ali, M. A. (1986). An improved interactive buckling analysis of thin-walled columns having doubly symmetric sections. *Int. J. Solids Structures* **22,** 429–443.

Sridharan, S. and Peng, M. H. (1989). Performance of axially compressed stiffened panels. *Int. J. Solids Structures* **25,** 879–899.